JOURNAL OF MATERIALS SCIENCE: MATERIALS IN MEDICINE 3 (1992) 33–42

Plasma spraying induced changes of calcium phosphate ceramic characteristics and the effect on *in vitro* stability

S. R. RADIN, P. DUCHEYNE
Department of Bioengineering, University of Pennsylvania, Philadelphia, PA 19104, USA

Plasma spraying is a commonly used technique to apply thin calcium phosphate ceramic coatings. Special consideration is given to retaining the original structure of CPC particles. However, changes are possible. Thus this study focused on plasma spraying induced changes in material characteristics of commercial coatings and their influence on *in vitro* dissolution. All analysed coatings were found to undergo significant plasma spraying induced changes in phase composition, crystal structure, and specific surface area. The phase transformations depended on the starting particle characteristics. Specifically, β-TCP transformed to α-TCP. HA was dehydroxylated and transformed to oxyhydroxyapatite (OHA), and partly decomposed to α-TCP and tetra calcium phosphate. These transformations lead to a considerable increase of *in vitro* dissolution rates at physiological pH.

1. Introduction

Calcium phosphate ceramic (CPC) coatings on metallic implants have a threefold possible beneficial effect: enhancement of bone formation rates [1], the ability of bonding to bone [2], and the reduction of metal corrosion product release [3]. Plasma spraying, electrophoretic deposition and sputter coating are various methods to achieve CPC deposition [4].

Plasma spraying takes CPC particles through high temperatures. Special consideration has therefore been given to retaining the original crystalline structure of the CPC particles. It has been indicated that plasma spraying of hydroxyapatite leads to retaining at least 95% of the coating in this crystalline structure. This conclusion was arrived at by using X-ray diffraction (XRD) [5, 6]. However, in some of our previous work, more significant plasma sprayed induced changes of the crystal structure, and a concomitant change of specific surface areas were documented [7]. Thus in this study we focus on plasma sprayed induced changes in material characteristics of a number of plasma sprayed CPC coatings obtained from commercial sources, and the influence of these changes on the *in vitro* stability of these coatings.

2. Methods and materials

Two types of starting CPC powders were used for the study: hydroxyapatite (HA) and β-tricalcium phosphate (β-TCP). Both the starting powders and the plasma sprayed coatings were obtained from commercial sources. The powder and coating nomenclature are listed in Table I. The starting HAM and β-TCPM had a mesh size of − 325, the starting HAF had a particle size 0.8 mm. The powders were sprayed onto Ti-6Al-4V alloy (ASTM F-137) flat or porous coated substrates. The average thickness of the CPC coatings was 70–80 μm. The porous metallic coatings were obtained with either − 60 + 80 mesh spherical commercial purity (c.p.) Ti powders (ASTM F-67) or orderly oriented wire mesh (OOWM) of mesh size 16 and with a 0.50 mm diameter wire [8].

The XRD patterns were obtained on a Rigaku diffractometer (D/Max II, Danvers, MA) with CuK_α radiation at 45 kV, 35 mA, a 2θ scanning rate of 1 deg min^{-1}. The instrument was equipped with a computerized diffractogram analyser. The infrared spectra were recorded on a Fourier transform infrared spectroscope (FTIR) Nicolet 5DXC (Madison, WI). The powders or scraped plasma sprayed coatings were analysed as 1% powder-KBr mixtures in the diffuse reflectance operational mode.

The morphology of the CPC plasma sprayed coatings either onto flat or porous surface was determined by using scanning electron microscopy (Philips, SEM 500, Eindhoven, The Netherland). Scanning Auger electron spectroscopy (SAEMS, PHI Microprobe 600, Perkin-Elmer, Eden-Prairie, MN) was used to analyse the plasma sprayed coating surface composition.

The assessment of stability of either the starting CPC or the plasma sprayed coatings was performed in simulated physiological, calcium and phosphate free solution (a 0.05 M tris (hydroxy) methylaminomethane-HCl buffer) at pH 7.3, 37 °C and 1 mg/1 ml mass to solution ratio, as described previously [9]. In brief, 10 mg of the powder, or metallic specimens with 10 mg of coating were immersed into 10 ml of the solution for periods of time ranging from 15 min to 24 h. For each period of time, four separate specimens were used. The vials were placed onto a shaker table.

The amount of released calcium was measured in triplicate by flame atomic absorption spectroscopy

0022–2461/92 $03.00 + .12

TABLE I Characteristics of the CPC before and after plasma spraying

Nomenclature	Crystal structure	Used method of analysis	Specific surface area ($m^2 g^{-1}$)
HAM st.[a]	stoichiometric HA	XRD FTIR	0.64
HAM PS[a]	OHA + α-TCP + tetra CP	XRD	0.29
β-TCPM st.[a]	stoichiometric β-TCP	XRD	1.19
β-TCPM PS[a]	α-TCP + β-TCP remain	XRD	0.79
HAF st.[b]	stoichiometric HA	XRD FTIR	0.13
HAF PS[b]	OHA + traces α-TCP and tetra CP	XRD FTIR	0.02
β-TCPD st.[c]	the same as β-TCPM	XRD	1.19
β-TCPD PS[c]	β-TCP + α-TCP	XRD	

Specimens kindly provided by [a] Miter, Warsaw, Indiana; [b] Feldmuhle, Plochingen, Germany (Osprovit); [c] De Puy, Warsaw, Indiana.

(AAS) (Perkin-Elmer, model 2380, Norwich, CT). The released phosphate was measured as the complex (molybdenum yellow) [10] in a UV-visible spectrophotometer (Biochrom, LKB 4053 Ultraspec, Cambridge, UK).

The specific surface areas were determined with the monolayer gas absorption technique (B.E.T.) by Micromeritics Co. (Norcross, GA) or Omicron Co. (Berkley Heights, NJ).

3. Results

3.1. Characteristics of the starting powders

Some characteristics of the starting CPC powders, including their crystal structures and specific surface areas are summarized in Table I. The starting HAM was stoichiometric, highly crystalline HA (as was confirmed by XRD and FTIR) with a low specific surface area (Table I). The FTIR spectrum of HAM (Fig. 1a) shows characteristic features of a completely crystallized HA, including well-pronounced OH^- peaks at 3572 and 633 cm^{-1}.

As follows from the FTIR analysis, the crystallization of the starting HAF was not complete (Fig. 2a). The spectrum shows a broad water band in the 3600–3000 cm^{-1} range; the OH^- bands at 3572 and 633 cm^{-1} are significantly smaller than those of the HAM spectrum. However, the specific surface area of HAF is very low. After calcination at 900 °C the FTIR spectrum of HAF is typical of stoichiometric, crystalline HA.

Starting β-TCPM powder was highly crystalline powder (as confirmed by XRD and FTIR) with a low specific surface area.

3.2. Characteristics of the plasma sprayed CPC

Some characteristics of the plasma sprayed coatings are also summarized in Table I. The FTIR spectra of HAM PS and HAF PS are shown in Figs 1b and 2b respectively. The XRD patterns of both plasma sprayed HAs and β-TCPs are represented in Fig. 3a to d.

Plasma spraying produced a dramatic change in the crystal structure of HAM as can be deduced from the XRD and FTIR results. The starting HA was transformed into a mixture of apatite, tetracalcium phosphate (tetra CP) and α-TCP as follows from the XRD pattern (Fig. 3a). Not only is the X-ray diffraction analysis important, in addition, the infrared spectra must be reviewed critically, since they bring out features (Fig. 1b) which cannot be observed by XRD. The OH^- bands at 3572 and 633 cm^{-1}, characteristic of HA, have fully disappeared. The 961 cm^{-1} band, characteristic of symmetric stretching of PO_4 group in HA, has disappeared, and two very weak bands at 960 and 946 cm^{-1} have appeared. Two medium intensity bands at 603 and 568 cm^{-1} and small shoulders can be seen in the bending vibration mode of the PO_4 group. All the above features can be assigned to oxyhydroxyapatite (OHA), of which the characteristic absorption bands were described before [11].

The FTIR spectrum of a single-phase OHA, which we produced by heating HA at 900 °C for 24 h *in vaco*, is shown for comparative purposes in Fig. 4b. This spectrum shows the following characteristic features: a very weak OH^- band at 3672 cm^{-1} and the absence of the hydroxyl band at 633 cm^{-1}, two medium intensity bands at 970 and 946 cm^{-1}; bands at 604, 582 and 568 cm^{-1} and a shoulder at 556 cm^{-1} in a bending vibration mode of the PO_4 group, and a medium intensity band at 481 cm^{-1}. Trombe and Montel [11] reported similar IR absorption bands for OHA. Specifically, l-bands at 965 and 935 cm^{-1}, η-bands at 600, 575, and 572 cm^{-1}, a shoulder at 560 cm^{-1}, and a 482 cm^{-1} band in the low energy region. They found that the above features are more pronounced with a higher degree of dehydroxylation.

The full absence of the OH^- absorption bands on the FTIR spectrum of HAM-PS indicates a high degree of dehydroxylation of the OHA. The small additional features in the FTIR spectrum of HAM-PS (Fig. 1b), especially in a low energy region, could be associated with tetra CP and α-TCP. Thus the combined XRD and FTIR analysis identifies the HAM-PS structure as a mixture of OHA, tetra CP and α-TCP.

The XRD pattern of the HAF subsequent to plasma spraying indicates a highly crystalline apatitic structure, with some α-TCP and tetra CP as revealed by their barely perceptible characteristic peaks (Fig. 3b). Whereas the XRD pattern would lead one to believe

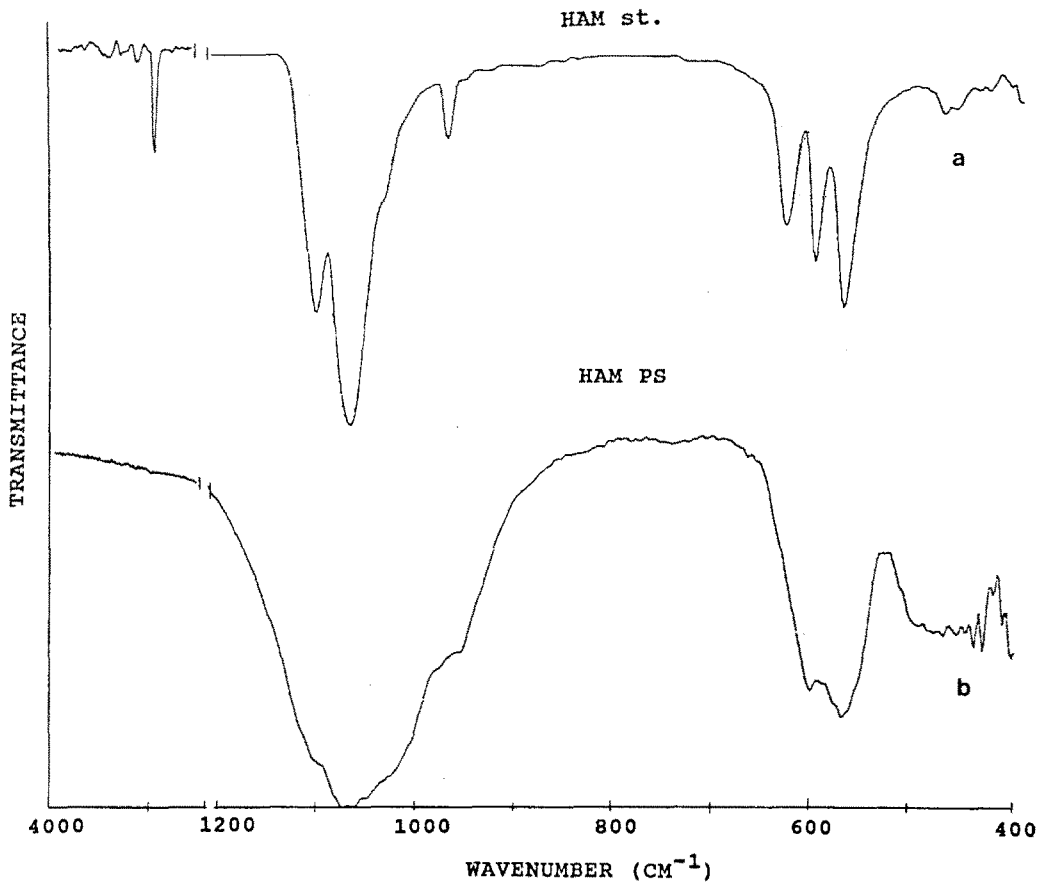

Figure 1 FTIR spectra of HAM starting (a) and HAM PS (b).

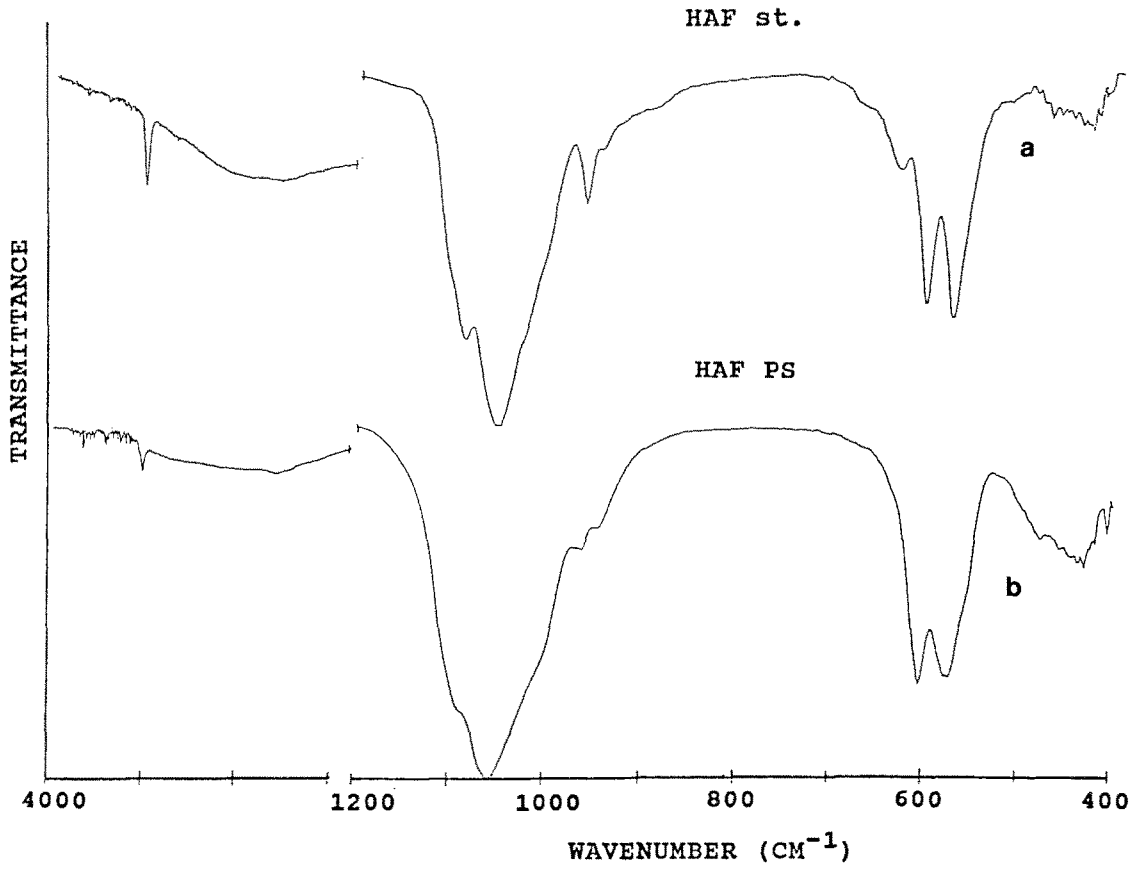

Figure 2 FTIR spectra of HAF starting (a) and HAF PS (b).

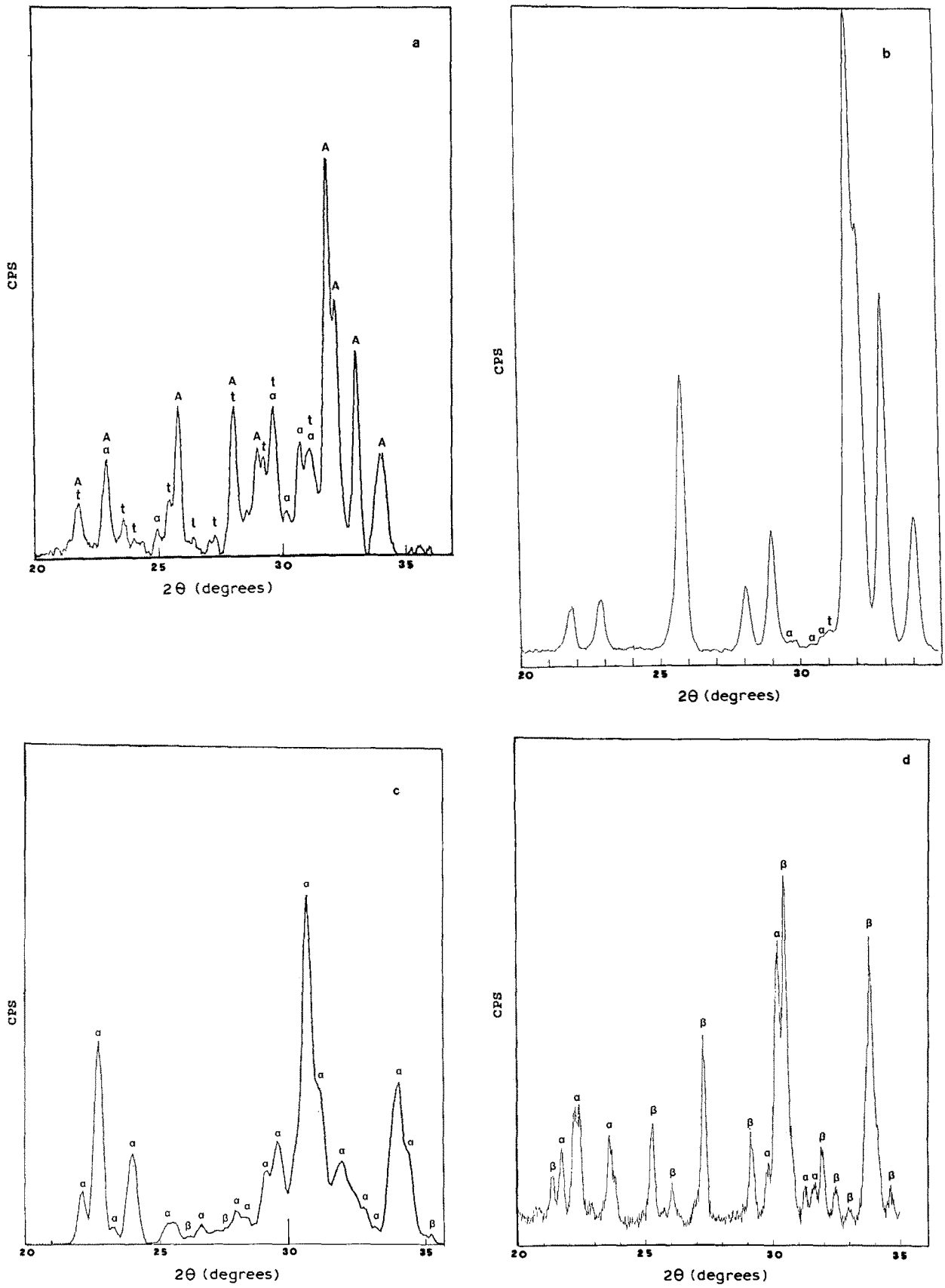

Figure 3 XRD spectra of plasma sprayed coatings: (a) HAM PS, (b) HAF PS, (c) β-TCPM PS, (d) β-TCPD PS.

that hydroxyapatite is largely retained, one must also consider the FTIR spectrum. After plasma spraying it differs significantly from that of the starting HAF, as can be seen by comparing Fig. 2a with Fig. 2b. The reduction of the 3572 cm^{-1} and the absence of the 633 cm^{-1} OH^- bands, the appearance of the weak bands at 962 and 948 cm^{-1} and the absence of the 961 cm^{-1} band are characteristic of the OHA structure. Thus the starting HAF underwent a partial dehydroxylation and transformation to OHA during the plasma spraying.

Plasma spraying transformed β-TCPM almost fully

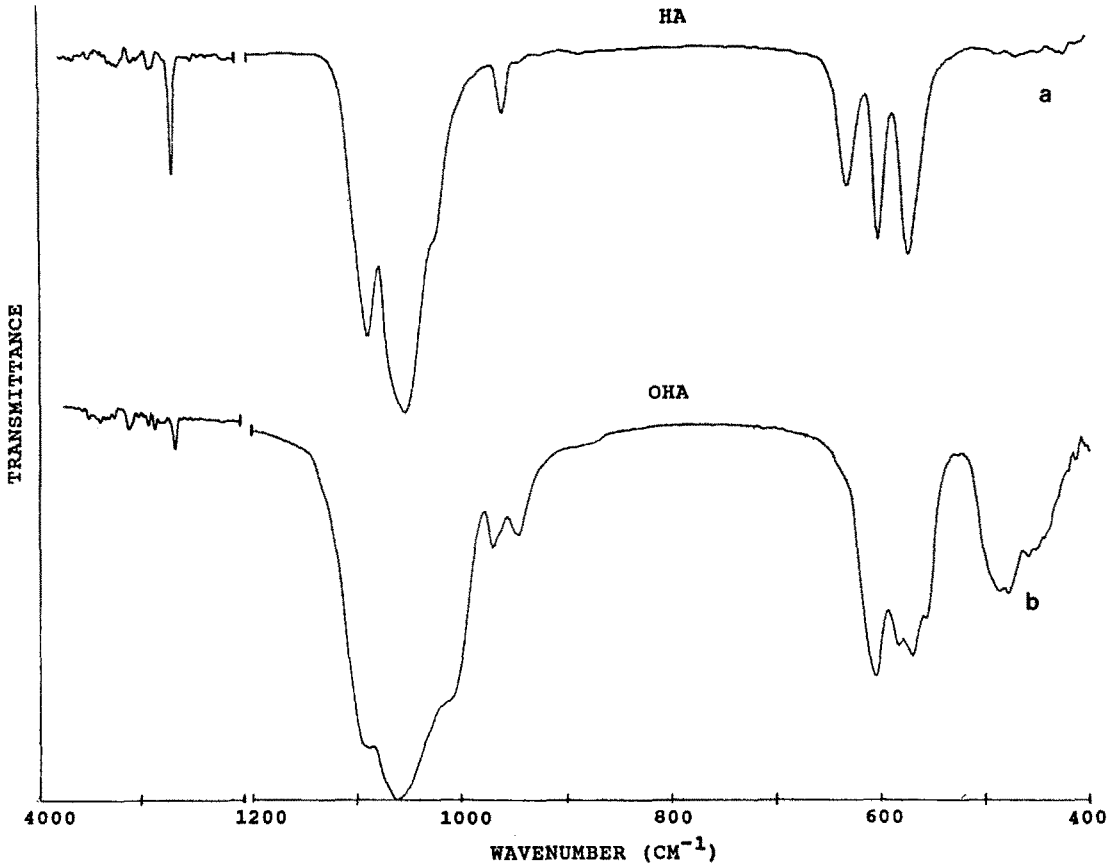

Figure 4 FTIR spectra of stoichometric HA (a) and OHA (b), produced by heating the HA at 925 °C for 24 h in high vacuum in a Pt crucible.

to α-TCP, with some β-TCP retained, as indicated by XRD spectrum of Fig. 3c. Broadness of the peaks indicates that the degree of crystallinity of β-TCPM PS decreased with respect to the starting highly crystalline powder. The β-TCPD was transformed into a mixture of α-TCP and β-TCP as confirmed by XRD analysis (Fig. 3d).

All the powders underwent reductions in specific surface areas, to a greater or lesser degree, due to plasma spraying (Table I).

3.3. SEM observations

The SEM micrographs of HAF PS coating onto a flat metal surface are represented in Fig. 5a, b. The small magnification view (Fig. 5a) shows a uniformly covered metal substrate. However, at larger magnifications (Fig. 5b) the coating is non-uniform since it consists of large smooth areas with a glassy appearance in combination with irregular shape ceramic chips and randomly distributed pores of different size; multiple cracking can be observed as well.

SEM micrographs of the HAF plasma sprayed coating onto the OOWM porous surface are shown in Fig. 6a, b. At small magnifications (Fig. 6a) the coating seems uniform on both the substrate and OOWM. However, higher magnifications reveal that the areas of the substrate adjacent to the wires, i.e. the corners

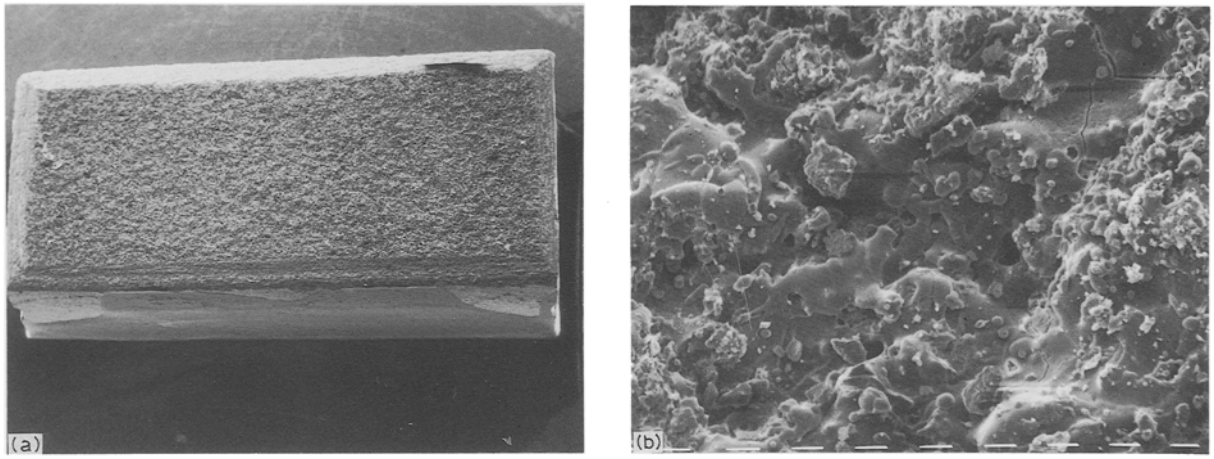

Figure 5 SEM micrographs of HAF PS coating onto a flat Ti alloy substrate: at magnification 10× (a), and details of microstructure at 640× (b).

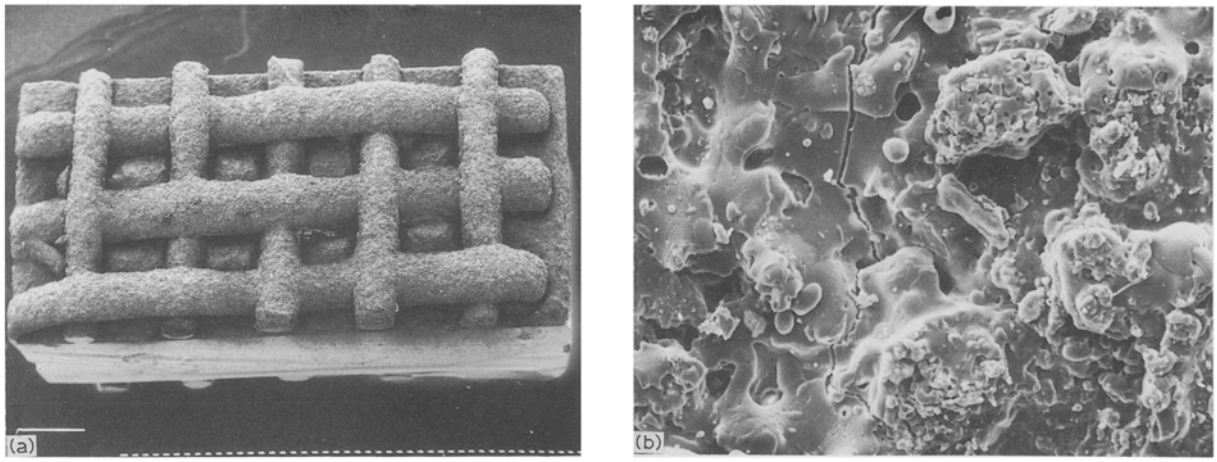

Figure 6 SEM view of the HAF PS coating onto porous OOOWM coated surface: at 10× (a), and details at 640× (b).

and the edges of the pores, were not coated, as well as the underside of the wires. The coating structure on the top of the wires (Fig. 6b) resembles that of the HAF PS coating onto the flat surface. Specifically, one sees large particles with a glassy and highly deformed appearance, ceramic chips, random pores, and cracking.

The starting HAF particles were relatively large 0.8 mm diameter particles. The SEM appearances suggest that some of the large particles apparently underwent surface melting when being taken through the high temperatures in the carrier gas. Furthermore, these melted surfaces were quenched at the moment of impact with resulting cracking and breaking of the particles.

3.4. Coating surface analysis

The SAEMS HAF PS coating surface survey revealed Ca, O and P peaks. A doublet low energy P peak was located at 92 and 109 eV. This observation corresponds to those reported for a phosphate group [12].

The Ca to P peak intensity ratio measured on the coating surface after 20 s of sputtering in the scan mode was found to be 6.0–6.2. The ratio is similar to that of a reference stoichiometric HA.

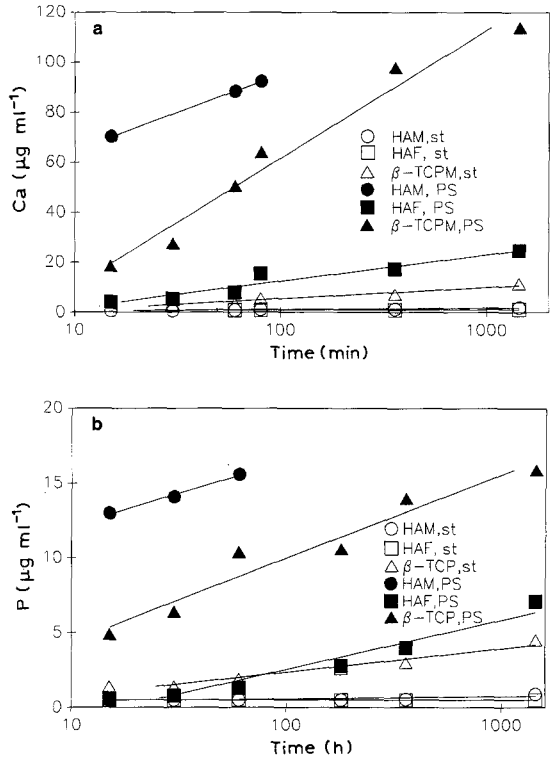

Figure 7 The Ca (a) and P (b) dissolution rates of the starting powders and plasma sprayed coatings in a 0.05 M tris buffer solution at pH 7.3 and 37 °C.

3.5. Dissolution behaviour of the CPC before and after PS

The concentrations of calcium and phosphate released from the CPC into the buffer solution for periods of time ranging from 15 min to 24 h are represented in Fig. 7a, b.

The starting HAM and HAF powders show the slowest dissolution rates as could be expected for stoichiometric well-crystallized HA with a low specific surface area. The starting β-TCPM shows a higher dissolution rate, since β-TCP is known to be more soluble than HA.

The dissolution rates of all plasma sprayed CPC, (either HAF-PS, HAM-PS or β-TCPM) were found to be significantly greater than those of the starting powders. Specifically, the concentration of calcium released from the immersed HAF-PS is an order of magnitude greater than that from the starting HAF. The concentrations of calcium released from either HAM-PS or β-TCPM PS appeared to be almost two orders of magnitude greater than those released from the starting powders. The HAM-PS and β-TCPM PS were found to be the most soluble. The dramatic increase in dissolution rates of the PS CPC occurs in spite of the decrease in their specific surface areas (Table I).

To demonstrate whether the transformation of HA to OHA or β-TCP to α-TCP can alter the dissolution behaviour of the starting CPC, we performed an analogous immersion test of OHA and α-TCP. OHA was obtained as described above. The α-TCP was

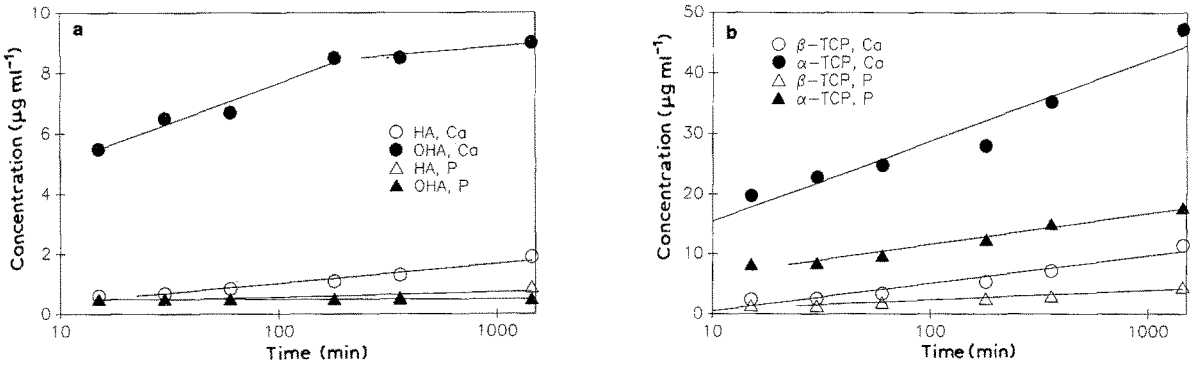

Figure 8 Changes in the dissolution rates of stoichiometric HA and β-TCP after full transformations to OHA (a) and α-TCP (b) respectively.

produced by heating β-TCPM at 1420 °C for 6 h. The crystal structures of these two CPC were confirmed by XRD.

The dissolution rates of the HA and β-TCP powders before and after transformation to OHA and α-TCP are represented in Fig. 8a and b respectively.

A major increase in solubility of both HA or β-TCP subsequent to the transformation to OHA or α-TCP respectively, was found. Both the starting and the transformed powders were single-phase CPC with the same Ca/P ratio, yet their solubility depended significantly upon their crystal structures.

4. Discussion

4.1. Phase transformations

All the studied HA or β-TCP PS coatings on metal surfaces, obtained from commercial sources, underwent, to different extents, plasma spraying induced changes, including changes in crystal structures, specific surface area and morphology. Furthermore, these changes affected the stability, or the dissolution behaviour of the ceramic.

According to requirements suggested in the literature, satisfactory coatings must be dense, adherent, and with structures not altered irreversibly by the coating technique [13]; HA coatings must consist of a 95% highly crystalline HA [5, 6]. To achieve these requirements, major efforts have been concentrated upon retaining the original structure and composition of CPC particles during plasma spraying. Retaining at least 95% of the original CPC crystal structure seems possible according to some sources [5, 6]; however, irreversible plasma spraying induced changes in crystal structures of plasma sprayed CPC have been found as well. Specifically, β-TCP transformation to "amorphous alpha phase" [14] and HA decomposition with TCP phase formation [15] have been reported.

We observed significant differences among the HA or β-TCP PS coatings obtained from different sources, although all the starting particles were stoichiometric, single-phase compounds. Specifically, plasma spraying decomposed HAM into a mixture of apatite with a large amount of α-TCP and tetra CP (Fig. 3a). In contrast, HAF-PS consisted of 95% apatite with barely detectable extra phases (Fig. 3b). The β-TCPM PS was almost fully transformed to α-TCP, while β-TCPD PS decomposed only partly and consisted of a mixture of β- and α-TCP (Fig. 1d).

In spite of the differences among the various PS coatings, similarities can also be noticed. All the studied coatings were well crystallized. Both HAM and HAF PS coatings underwent dehydroxylation and decomposition to a mixture of apatite with α-TCP and tetra CP. Both β-TCPM and β-TCPD coatings transformed to α-TCP subsequent to PS. Thus the differences are primarily related to the degree of transformation.

The above plasma spraying induced transformations of either HA or β-TCP can be expected, because plasma spraying takes the particles through high temperatures. At temperatures above 1050 °C there exists equilibrium for HA with TCP and tetra-CP as follows [16]:

$$Ca_{10}(PO_4)_6(OH)_2 \rightleftharpoons 2Ca_3(PO_4) + Ca_4P_2O_9 + H_2O$$

The β-modification of TCP is stable at temperatures up to 1120 °C; in the range from 1120 °C and up to 1470 °C the α-modification of TCP is stable [17]. The transformation temperatures depend on partial water pressure, impurities and stoichiometry. In case of CPC applied as coatings on metal surface other factors may be involved shifting the above reaction toward destabilization of HA or lowering the β-TCP to α-TCP transition temperature. For instance, this might be a phenomenon similar to the effect of a titanium substrate upon sintering β-TCP: it was found that it promoted β- to α-TCP transformation [9].

There are several techniques to prevent the decomposition of HA or β-TCP during plasma spraying, such as using large starting particles, varying the PS atmosphere, and controlling plasma spraying parameters which minimize time of flight and temperature. This may lead to retaining a 95% apatitic structure as in the case of HAF PS. However, dehydroxylation of HA can hardly be prevented at the high plasma spraying temperatures. There is a likely dehydroxylation, according to the reaction:

$$Ca_{10}(PO_4)_6(OH)_2 \rightleftharpoons Ca_{10}(PO_4)_6(OH)_{2-2x}O_x[\ ]_x + xH_2O,$$

where [ ] is a vacancy.

It is important to point out that XRD analysis does

not reveal the dehydroxylation. The XRD patterns of the main components of both HA and PS are apatitic structure patterns (Fig. 3a, b). If the structural characterizations were only based on XRD analysis, one could conclude to a hydroxyapatite structure. Yet, the recorded IR spectra of the HA PS do not correspond to that of HA, but resemble that of OHA which was first described by Trombe and Montel [11]. They indicated that it is hardly possible to obtain stoichiometric oxyapatite stable in air at room temperature. One obtains solid solutions of HA and oxyapatite, with compositions closer to oxyapatite. A composition of a slightly hydroxylated OHA, i.e. one which does not produce the 3572 cm^{-1} OH^- band in the IR spectrum, corresponds to the formula

$$Ca_{10}(PO_4)_6(OH)_{0.5}O_{0.75}[\ ]_{0.75}.$$

Upon hydroxylation, i.e. the increase of water content in the lattice of OHA, the IR spectrum gradually changes toward the one of HA. Specifically, a gradual increase of intensity of the 3572 and 633 cm^{-1} OH^- bands occurs with increasing hydroxylation [11].

The information contained in the characteristic spectral features of the OH^- group leads to the identification of important structural characteristics which cannot be made by XRD. In addition, the FTIR spectra also bring out features in the PO_4 bands energy region with structural information impossible to obtain by XRD. Two weak bands at 970 and 946 cm^{-1} replace the symmetric stretching band of the PO_4 group of HA at 961 cm^{-1}. Small extra bands for a bending mode of vibration (in the range from 604 to 556 cm^{-1}) and a medium intensity band at 480 cm^{-1} appear (Fig. 4a, b). In general, the number of bands attributable to PO_4 groups in apatites containing bivalent ions (O^{2-}, CO_3^{2-}, S^{2-}), is greater than the theoretical number for a crystal with hexagonal symmetry and spatial group $P6_3/m$. In the case of OHA (or other apatites with bivalent ions), a bivalent ion (O^{2-}) and a vacancy substitute for two monovalent ions. The substitution leads to a distortion of the symmetry. Since XRD shows a hexagonal symmetry there must be statistical disorder of the bivalent ions and vacancies along the *c*-axis. The distortion, however, affects the infrared spectrum: even though the phosphate groups occupy identical positions in the HA or OHA lattice, there is a difference in terms of location with regard to the bivalent ions or vacancies in the lattice of OHA [11].

Plasma spraying also affects coating morphology and microporosity. We found that plasma spraying leads to a reduction in specific surface area for all of the studied coating apparently due to a combined effect of heat and impact. Plasma spraying changes the morphology of particles. Specifically, the HAF PS coating at high magnification appears to be a combination of large highly deformed particles with a glassy appearance, ceramic chips, randomly distributed pores, and cracks. These cracks could lead to local stress concentration and a crevice-like conditions which would result in mechanical and physico-chemical instability of the coatings.

The stoichiometry of the CPC does not appear to be affected by plasma spraying. The Ca/P ratio of the coatings, estimated by measuring the Ca/P Auger peak intensity ratio on the surface of HAF PS, was found to correspond to that of stoichiometric HA used as a reference. Thus plasma spraying does not seem to change stoichiometry of the outer layer of the coatings. It is this layer which determines the initial solid–solution interfacial reactions and biological response upon implantation.

4.2. *In vitro* stability

Controversial reports on the degree of plasma sprayed coating resorption [14, 18–20] suggest dependency on the process parameters. In the present study we determined the dissolution rates of the plasma sprayed coatings in calcium and phosphate free buffer solution at physiological pH. The dissolution rates of all the studied ceramic coatings were found to be greater than those of the starting particles. Both, the initial dissolution rates, as well as the Ca and P concentrations in solution appeared to increase. The observed increase in the dissolution rates occurs in spite of the plasma sprayed induced decrease in specific surface areas.

The dissolution rates of both HAM PS and HAF PS exceeded that of starting β-TCP which is known as a soluble, metastable and resorbable member of the CPC family. Even HAF PS, which is actually 95% apatite, was found to be more soluble than the starting β-TCP. The dissolution rates of the HAM PS and β-TCPM PS were found to be significantly greater than the starting HAM and β-TCP (Fig. 7a), and both showed the greatest solubility among the studied compounds, either starting or plasma sprayed. The dissolution rates of both studied β-TCP PS were found significantly enhanced compared with that of the starting powders.

Among the main factors which have been forwarded to explain solubility of CPC at constant pH are the Ca/P ratio [16], porosity and microporosity [21] (specific surface area). Since these factors are either unchanged, or work oppositely, the main factor to consider is the plasma spraying induced phase transformations. Specifically, a greater solubility of HAF-PS compared with the starting HAF is apparently related to the transformation of HA to OHA. Furthermore, important increases in solubility occur when single phase HA or β-TCP decompose into α-TCP containing mixtures, OHA + α-TCP + tetra CP, or α-TCP + β-TCP respectively. The dissolution experiment with single-phase OHA and α-TCP made by us proves that the transformations of HA into OHA and β-TCP into α-TCP lead in fact to significant increases in the dissolution rates (Fig. 8a, b).

The solubility of OHA was expected to be high on the basis of thermodynamic considerations [22]. The current data show that the Ca release rate from OHA in a Ca-free buffer solution at pH 7.3 is comparable with that of β-TCP (Fig. 8a). The higher solubility of OHA is probably related to the distortion of the hexagonal symmetry caused by the bivalent ions

(O^{2-}) and vacancies. A crystal structure disorder following from the high temperature rearrangements occurring during β- to α-TCP transformation is apparently responsible for the greater solubility of α-TCP.

Significant rates of resorption and degradation of plasma sprayed CPC coatings reported in a number of studies [20, 23, 24] can be related to the herewith reported spraying induced enhancement of *in vitro* dissolution rates. Specifically, the observed 10 μm wk^{-1} resorption rate of plasma sprayed β-TCP coating [23] may be explained by transformation of the original structure to α-TCP, as reported by the authors. In a later report [14] a group of authors from the same laboratory argued that the resorption rate of β-TCP PS was not as great as was reported before [23]; however, they did not mention the actual structure of the coating in this more recent study.

The resorption rate of a plasma sprayed HA coating consisting of "over 98% highly crystalline HA as confirmed by XRD" was found to be 50 μm in few first months [20]. However, since dense HA is generally described as "non-resorbable", we can assume that the reported significant resorption of the coating with 98% HA was probably related to dehydroxylation and transformation of insoluble HA to metastable OHA during plasma spraying. The 2% remaining unidentified structural components, which were apparently α-TCP and tetra CP can also lead to an additional enhancement of resorbability.

Plasma sprayed HA and β-TCP showed no significant difference in degradation rates in Ringer's and saline [24]. Although the authors did not report on the resultant coating structures, decomposition of HA with a formation of α-TCP and transformation of β- to α-TCP which are likely to occur during plasma spraying may have lead to an almost similar instability of the HA and β-TCP PS coatings [24].

5. Conclusions

All the commercially obtained coatings underwent significant plasma sprayed induced changes in crystal structure, phase composition, specific surface area and morphology. The phase transformations depended on the starting particle characteristics. Specifically, the starting β-TCP transformed to variable concentrations of α-TCP. The starting HA was dehydroxylated and transformed to OHA, and partly decomposed to α-TCP and tetra CP.

HA and OHA can not easily be differentiated by using XRD, however, they can easily be identified as different compounds by using infrared analysis.

The plasma sprayed phase transformations produce significant increases in *in vitro* dissolution rate of both plasma sprayed HA and TCP coatings. All HA coatings including the coating with a 95% highly crystalline apatitic structure showed significantly enhanced dissolution rates.

Acknowledgements

This work was supported by NSF, ECE 85-15031. Specimens were kindly provided by the companies listed in Table I.

References

1. P. DUCHEYNE, L. L. HENCH, A. KAGAN, M. MARTENS, A. BURSSENS and J. C. MULIER, "The effect of hydroxyapatite impregnation on skeletal bonding of porous coated implants", *J. Biomed. Mater. Res.* **14** (1980) 225–237.
2. M. JARCHO, "Calcium phosphate ceramics as hard tissue prosthetics", *Clin. Ortho. Rel. Res.* **157** (1981) 259–277.
3. P. DUCHEYNE, K. HEALY, "The effect of plasma sprayed calcium phosphate ceramic coatings on the metal ion release from porous titanium and cobalt chromium alloys", *J. Biomed. Mater. Res.* **2** (1988) 1137–1163.
4. W. LACEFIELD, S. METSGER, N. BLUMENTHAL, P. DUCHEYNE, J. DAVIES, J. KAY, J. STEVENSON and R. SALSBURY, "*In vitro* analysis of coatings", *J. Appl. Biomater.* **1** (1990) 84–87.
5. J. F. OSBORN, "Assessment of the biomechanical quality of the newly formed bone in micro regions following hydroxyapatite ceramic implantation", in "Bioceramics", Vol. 1, edited by H. Oonishi, H. Aoki and K. Sawaki (Ishiyaku Euro America, Kyoto, Japan, 1989) p. 388.
6. H. OONISHI, M. YAMAMOTO, H. ISHIMARU, E. TSUJI, S. KUSHITANI, M. AONO and Y. UKON, "Comparisons of bone ingrowth in porous Ti-6Al-4V beads uncoated and coated with hydroxyapatite", in "Bioceramics", Vol. 1, edited by H. Oonishi, H. Aoki and K. Sawaki (Ishiyaku Euro America, Kyoto, Japan, 1989) p. 400.
7. P. DUCHEYNE, J. CUCKLER, S. RADIN and E. NAZAR, "Plasma sprayed calcium phosphate lining on porous metal coatings for bone ingrowth", in "Handbook of bioactive ceramics", edited by T. Yamamuro, L. L. Hench and J. Wilson (CRC Press, Boca Raton, FL), in Press.
8. P. DUCHEYNE and M. MARTENS, "Orderly oriented wire meshes (OOWM) as porous coatings on orthopaedic implants. I. Morphology, clinical materials", **1** (1986) 59–67.
9. P. DUCHEYNE, S. RADIN, J. C. HEUGHEBAERT and M. HEUGHEBAERT, "Calcium phosphate ceramic coatings on metallic porous surfaces. The effect of structure and composition on the electrophoretic deposition, vacuum sintering, and *in vitro* dissolution behavior", *Biomaterials* **11** (1990) 244–254.
10. J. K. HEINOKEN and R. J. LAHTI, "A new and convenient colorimetric determination of inorganic orthophosphate and its application to the assay of inorganic pyrophosphatase", *Anal. Biochem.* **113** (1981) 313–317.
11. J.C. TROMBE and G. MONTEL, "Some features of the incorporation of oxygen in different oxydation states in apatitic lattice", *J. Inorg. Nucl. Chem.* **40** (1978) 15–21.
12. W. VAN RAEMDONCK, P. DUCHEYNE and P. MEESTER, "Auger electron spectroscopic analysis of hydroxyapatite coating on titanium", *J. Amer. Ceramic Soc.* **67** (1984) 381–384.
13. W. R. LACEFIELD, "Hydroxyapatite coatings in bioceramics: materials characteristics versus *in vivo* behavior", edited by P. Ducheyne and J. Lemons. *Ann. N.Y. Acad. Sci.* **523** (1988) 72.
14. J. C. CHAE, J. P. COLLIER, M. B. MAYOR and V.A. SUPRENANT, "Efficacy of plasma sprayed tricalcium phosphate in enhancing the fixation of smooth titanium intramedullary rods", in "Bioceramics: material characteristics versus *in vivo* behavior", edited by P. Ducheyne and J. Lemons. *Ann. N.Y. Acad. Sci.* **523** (1988) 81.
15. D. P. RIVERO, J. FOX, A. K. SKIPOR, R. M. URBAN and J. O. GALANTE, "Calcium phosphate-coated porous titanium implants for enhanced skeletal fixation", *J. Biomed. Mater. Res.* **22** (1988) 191–201.
16. W. VAN RAEMDONCK, P. DUCHEYNE and P. DE MEESTER, "Calcium phosphate ceramics", in "Metal and ceramic biomaterials", Vol. 2, edited by P. Ducheyne and W. Hasting (CRC Press, Boca Raton, FL, 1984) ch. 6, p. 149.
17. J. C. HEUGHEBAERT, and G. BONEL, "Composition, structure and properties of calcium phosphates of biological

interest", in "Biological performance of biomaterials", edited by P. Christel, A. Meunier and A. J. C. Lee (Elsevier, Amsterdam, 1986) p. 9.
18. R. G. T. GEESINK, K. De GROOT and C. KLEIN, "Chemical implant fixation using hydroxyapatite coatings", *Clin. Orthop. Rel. Res.* **225** (1987) 147.
19. S. COOK, K. THOMAS, J. KAY and M. JARCO, "Hydroxyapatite coated titanium for orthopaedic applications", *Clin. Orthop. Rel. Res.* **232** (1988) 225.
20. J. F. OSBORN, "Bonding osteogenesis under loaded conditions – the histological evaluation of a human autopsy specimen of a hydroxyapatite ceramic coated stem of a titanium hip prosthesis", in "Bioceramics", edited by H. Oonishi, H. Aoki and K. Sawai (Kyoto, Japan, 1989) p. 388.
21. K. De GROOT, "Effect of porosity and physicochemical properties on the stability, resorption and strength of calcium-phosphate ceramics", in "Bioceramics: materials characteristics versus *in vivo* behavior", edited by P. Ducheyne and J. Lemons. *Ann. N.Y. Acad. Sci.* **523** (1988) 227.
22. F. C. M. DRIESSENS, "Physiology of hard tissues in comparison with solubility of synthetic calcium phosphates", in "Bioceramics: materials characteristics versus *in vivo* behavior", edited by P. Ducheyne and J. Lemons. *Ann. N.Y. Acad. Sci.* **523** (1988) 131.
23. C. K. HANES, J. P. COLLIER and M. B. MAYOR, "The use of tricalcium phosphate to provide enhanced early fixation of porous coated implants", in Trans. 11th. Ann. Soc. Biomat. Mtg, 1985, p. 176.
24. D. A. TESKE, M. B. MAYOR, J. P. COLLIER and V. A. SURPRENANT, "A comparative study of the effectiveness of plasma sprayed hydroxyapatite and tricalcium phosphate coatings in enhancing the fixation of smooth Ti-6Al-4V implants", in Trans. 35th Ann. Mtg, ORS, 1989, p. 333.

Received 29 August 1990
and accepted 11 January 1991